Chapter

Antennas for UWB Applications

Symeon Nikolaou and Abdul Quddious

Abstract

"Antennas for UWB Applications" chapter deals with an overview of ultra-wideband (UWB) antennas used for different applications. Some fundamental and widely used radiators, such as fat monopole, microstrip-fed and coplanar waveguide (CPW)-fed slot antennas, and tapered end-fire antennas are presented. Selected antenna designs are presented in relation to the UWB applications and their dictating radiation and operation principles. The demonstrated UWB antennas include antennas for handheld devices used for personal area network (PAN) communications; antennas for localization and positioning; UWB antennas for radio-frequency identifications (RFIDs); radar antennas for through-wall imaging, for ground-penetrating radar (GPR), and for breast tumor detection; and more generally, UWB antennas used for sensing. For some of the aforementioned applications, UWB antennas with special characteristics are needed, and they are presented and associated with the relevant applications. These include reconfigurable UWB antennas, metamaterial-loaded UWB antennas, and conformal UWB antennas. The usefulness of these special characteristics in comparison with the claimed advantages is critically evaluated. For the UWB applications presented in the chapter, one type or UWB antenna is recommended.

Keywords: UWB antennas, reconfigurable UWB antennas, UWB-RFID, conformal UWB antennas, microwave imaging, breast tumor detection

1. Introduction

There is a wide range of fundamentally different applications that use UWB antennas, and as a general approach, different customized antennas are needed depending on the desired radiation characteristics. The most common applications are data communication, localization and identification, and radar and sensing applications.

UWB communications have inherently very wide bandwidth in which, based on Shannon's theorem, these systems can support high data rates. Therefore, UWB transceivers are used for the transmission of high data rate, wireless communications, which are often used for PAN communications. One popular commercial application is the wireless USB (WUSB) which is designed to achieve 480 Mbit/s at distances up to 3 m and 110 Mbit/s at up to 10 m. PAN communications involve mobile handheld devices, in which case the used antennas should preferably have omnidirectional patterns with compact size and planar designs [1, 2]. Considering that UWB spectrum is shared with other technologies and standards such as the 3.6 GHz IEEE 802.11y wireless local area networks (WLAN) (3.6575–3.69 GHz), 4.9 GHz public safety WLAN (4.94–4.99 GHz), and 5 GHz IEEE 802.11a/h/j/n WLAN (5.15–5.35, 5.25–5.35, 5.47–5.725, 5.725–5.825 GHz), all operating within

the Federal Communication Commission (FCC) designated UWB band, of 3.1–10.6 GHz, the design of reconfigurable notch-band antennas has attracted a lot of attention [3–5] since they can potentially filter out the unwanted interferer.

UWB technology is used for positioning and location tracking. In the general principle, a UWB interrogator transmits a signal which is reflected by UWB tags which are identified, and depending on the number of interrogators and the utilized software, the position of the specific tag can be defined with relatively high accuracy. Currently there are companies such as UWINLOC which offer integrated solutions for smart and efficient asset management through real-time location systems (RTLS) by combining UWB technology with Internet of things (IoT) principles. Depending whether the UWB antenna is intended for the interrogator [6] or the UWB-RFID tag [7], the radiation characteristics and the size constraints may vary significantly. While the interrogator can combine multiple elements in arrays with beam-forming capabilities, the RFID tags need to be compact, lightweight, omnidirectional, and mostly, low-cost. In order to meet this last requirement, chipless UWB RFIDs [8] are used since they can be easily and massively manufactured on demand using additive fabrication technology.

"Radar devices" involve a wide variety of highly specialized applications for which UWB technology and UWB antennas are widely used even if many of the preferred UWB antennas radiate on different frequencies than the FCC designated 3.1–10.6 GHz band. Ground-penetrating radars (GPR) is one such application for which radars are used either to detect objects buried in the ground [9], to estimate soil characteristics (i.e., moisture) [10], or even to detect living beings trapped in ruins, after a physical disaster such as an earthquake or a hurricane. For this latter case, a more sophisticated radar—through-wall imaging radar—can also be used. Through-wall imaging systems are usually limited for use from law enforcement units, to monitor the position and movements of potentially dangerous targets [11], or even as airport security measure, in order to identify concealed weapons [12]. Microwave imaging [13] which is a more general category, under which the two aforementioned applications can be classified, includes the medical microwave imaging category which has attracted a lot of attention in the recent years. Medical microwave imaging is widely used for breast tumor detection [14, 15], and after several research efforts that investigated conformal UWB arrays [16, 17] and image reconstruction algorithms, several university spin-offs and other private companies proceeded with the implementation of commercial devices that were cleared for clinical studies with human subjects [18, 19]. These devices include both large-size devices facilitated at hospitals [20] and lightweight wearable devices for individual use at home [21].

This chapter presents an indicative list of UWB antennas which can be used for data communications, RFIDs used for identification and localization, and UWB antennas used for sensing and radar applications.

2. UWB antennas for wireless communications

"UWB communication systems" include communications which serve a variety of purposes. In a more loose definition, ultrawideband communication system is a system that requires more than 500 MHz bandwidth. Consequently, applications can be found in several subsections of the electromagnetic spectrum, starting from the UHF band all the way up to mm wave and sub-mm wave frequencies. This section focuses on UWB antennas for communications within the FCC designated UWB frequency range, 3.1–10.6 GHz. When UWB communications started to concentrate increased researchers' attention, (First International Conference

on UWB-ICUWB, in 2001, is considered a milestone), in the early 2000, the used antennas were rather large in size. Some of the earlier UWB antenna versions included self-complementary antennas which are frequency independent (spiral antenna) or wideband dipoles [22]. For the use of UWB technology for mobile handheld devices, the large antenna size was becoming a limiting factor. Consequently, size reduction became one of the primary objectives of the UWB antenna designers.

In the next years, self-complementary antennas and end-fire antennas were replaced with multiple resonator antennas. The design approach is to create several resonances on the S_{11} which are distributed along the 3.1–10.6 GHz frequency range. As a result, the reflection coefficient is "pushed" lower than −10 dB conventional matching threshold which is widely used as the "good matching" criterion. The existence of radiating segments of specific size causes the creation of the resonances in the reflection coefficient, and the size variation of the physical size of the resonators results in the corresponding resonance shift in frequency. **Figure 1** illustrates a series of multiple resonator antennas which progressively limit their overall (board) size. The antennas are CPW-fed, and the central (signal) conductor is linearly tapered to improve the matching. Details about the design and performance of the depicted antennas can be found in [2]. It has been shown that the transition from the conventional transmission line to the radiator and the ground size both affect the overall matching and consequently the radiation efficiency of the UWB antenna and should be considered by antenna designers as inherently integrated parts of the radiator itself. **Figure 1a** demonstrates an uneven U-shaped stub, radiating inside an elliptical slot. Under the observation of the limited effect of the slot on the matching, the slot was removed, and an additional linear segment was added on
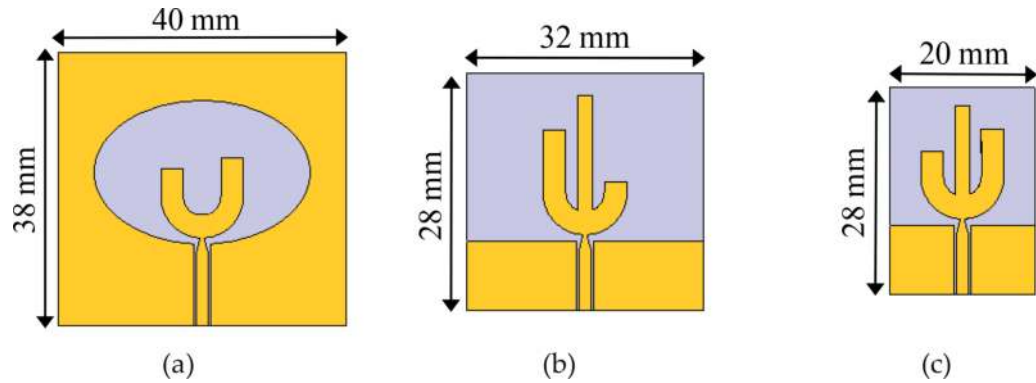

Figure 1.
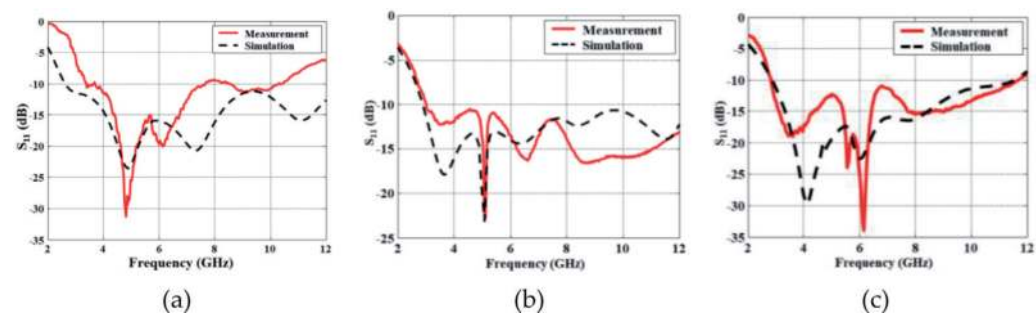*CPW-fed (a) elliptical slot, (b) cactus and (c) compact-cactus UWB antenna.*

Figure 2.
Simulated and measured S_{11} for (a) CPW-fed slot antenna, (b) cactus antenna, and (c) compact-cactus antenna [22].
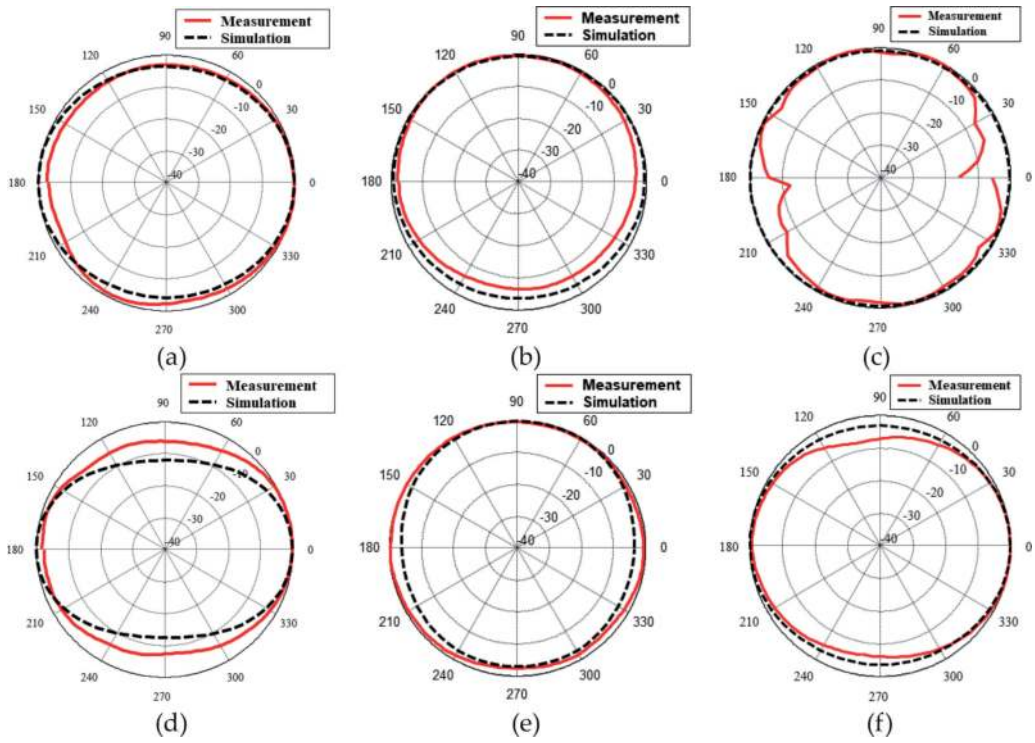
Figure 3.
Simulated and measured H-plane radiation patterns of (a) CPW-fed slot antenna, (b) cactus antenna, and (c) compact-cactus antenna at 5 GHz and (d) CPW-fed slot antenna, (e) cactus antenna, and (f) compact-cactus antenna at 9 GHz [22].
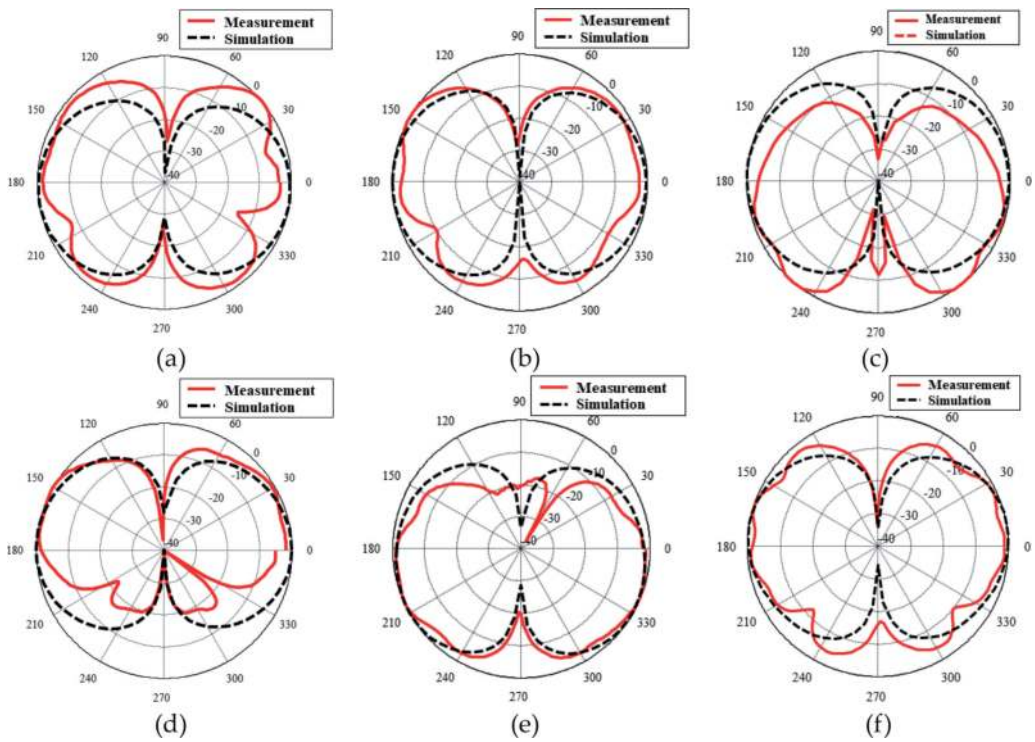
Figure 4.
Simulated and measured E-plane radiation patterns of (a) CPW-fed slot antenna, (b) cactus antenna, and (c) compact-cactus antenna, at 5 GHz, and (d) CPW-fed slot antenna, (e) cactus antenna, and (f) compact-cactus antenna, at 9 GHz [22].

the U-shaped stub, converting it into a "cactus-shaped" radiator consisting of three linear segments (**Figure 1b**). The last iteration presents a variation of the cactus-shaped radiator, the "compact cactus," with smaller RF-ground patches (**Figure 1c**) and further decreased overall size. **Figure 2** presents the reflection coefficient plots where the resonances are distributed along the entire UWB frequency band.

Although the elliptical slot does not affect the matching significantly, it has more profound impact on the resulted radiation patterns. The removal of the slot modifies the radiation patterns to rather omnidirectional patterns along the H-plane (**Figure 3**), while the E-plane (**Figure 4**) patterns are characterized by a null in the direction of the feeding line. Several other published research works demonstrated the attractive features and the effectiveness of the so-called fat monopole or the elliptical disc and its variations, as UWB radiator, and it became one of the most widely used UWB antenna types, for mobile handheld devices.

3. Reconfigurable UWB antennas for wireless communications

UWB systems share the same spectrum with several other narrowband wireless systems which use sub-bands inside the 3.1–10.6 GHz range. The FCC mask limits the UWB EIRP to −41.3 dBm/MHz, which means that UWB signals are rather weak, to degrade the performance of the narrowband systems, significantly. UWB signals are considered white noise for narrowband systems. On the other hand, UWB systems suffer from the strong interfering signals which are used from the narrowband systems. In order to reduce the received noise level and improve the associated SNR, UWB antennas are designed with notch bands, which effectively filter out the received signals at the frequencies used from a competing narrowband system. Ideally these notch bands should be reconfigurable, in other words to appear when an interfering signal is detected and to disappear when no such signal is detected. Generally, notch bands are caused from added resonators which are placed on the radiator, or the feeding line, or even the RF ground patches. **Figure 5** presents a microstrip-fed monopole with three pairs of added resonators which cause three notch bands on the reflection coefficient [23]. Each pair of resonators is designed to cause a notch band at a desired frequency. Specifically, the two stepped λ/4 open stubs cause the notch at the WiMAX (3.5 GHz) band; the two capacitively loaded loops (CLLs) on the ground patch cause the notch at the WLAN (5.8 GHz) band, and the pair of linear λ/2 segments, printed on the back side of the radiator, causes the notch at 8.87 GHz. The use of three different pairs of resonators allows the control of the notch bands independently. The effect of the resonators can be made reconfigurable if suitable switches are used at the right place. **Figure 5b** shows that if the λ/4 open stubs are disconnected (switch in off state), the frequency notch disappears (blue solid line). In **Figure 5c** the reflection coefficient of the UWB antenna is presented when the switch on the CLL is in either on or off state. With the switch in off state, the WLAN notch exists and filters out the undesired high-power signal, while when the switch is in on state, the effect of the CLL is canceled, and as a result the UWB antenna radiates efficiently at the WLAN band. Finally, when the switch separating the λ/2 linear segment into two unequal parts (**Figure 5d**) is set to off state, it causes the cancelation of the notch at 8.8 GHz.

Depending on the geometry of the resonator, a variety of electronic switches can be implemented. **Figure 6** presents three implemented UWB antennas [24–25], with reconfigurable notch bands at the WLAN band (5.8 GHz) which use a single resonator instead of a pair of resonators and, consequently, only one switch to implement the notch reconfigurability feature. A microstrip-fed monopole with a J-shaped stub inside a rectangular slot is presented in **Figure 6a**, where the J-shaped
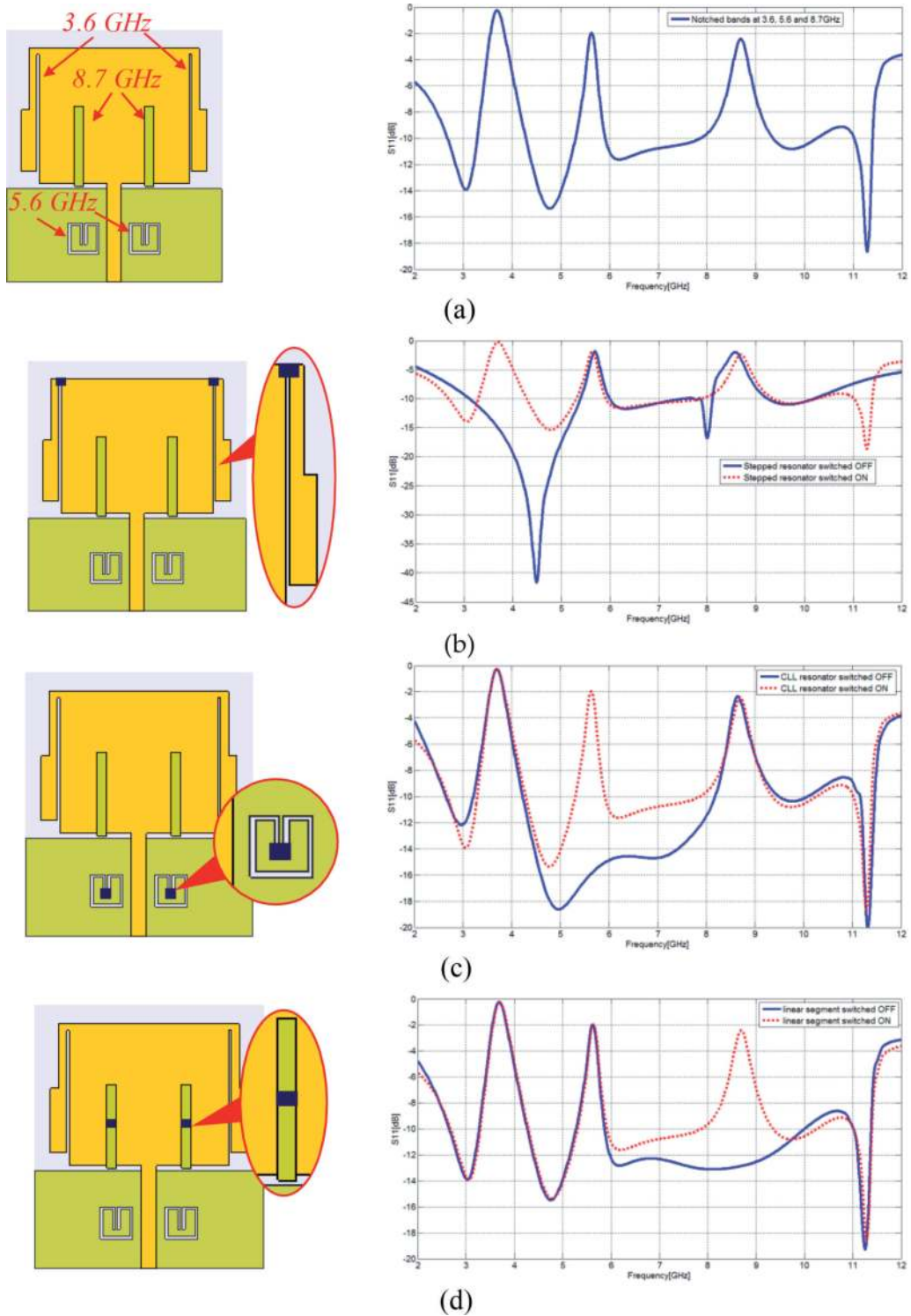
Figure 5.
Simulated S_{11} microstrip-fed UWB (a) monopole with three pairs of resonators (b), stepped λ/4 open stubs (c), CLL resonators, and λ/2 parasitic linear segments (d).

stub is connected and disconnected to the radiator, using a PIN diode switch. The J-shaped stub causes the notch, but when the diode is set to off state, the stub is disconnected, and the frequency notch is suppressed. In a similar design, the dynamically reconfigurable UWB antenna presented in **Figure 6b** uses a low-power field-effect transistor as switch (FET switch) to connect and disconnect the linear
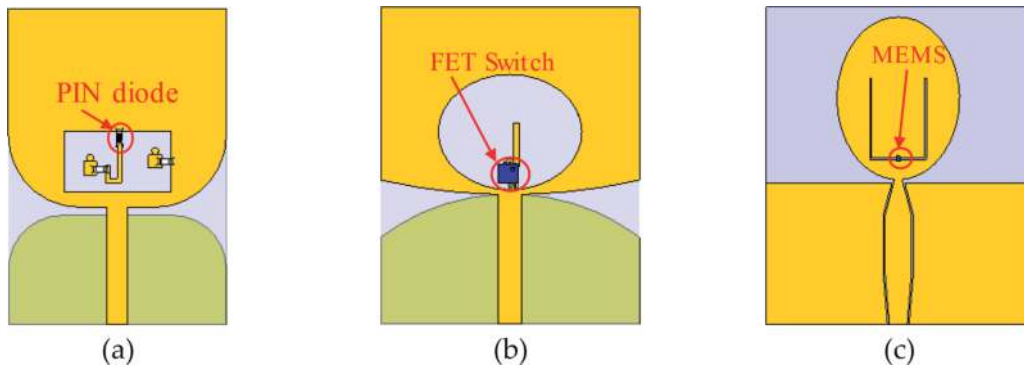
Figure 6.
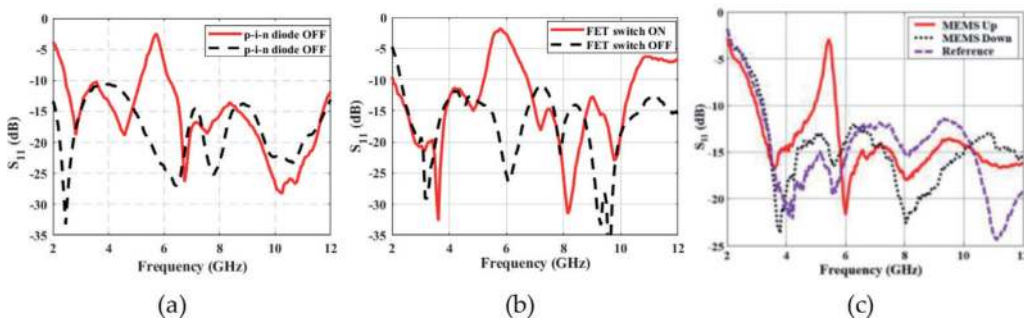*Reconfigurable UWB antennas with (a) PIN diode, (b) FET switch, and (c) MEMS.*

Figure 7.
Measured S_{11} of three different reconfigurable UWB antennas with (a) PIN diode, (b) FET switch, and (c) MEMS.

segment inside the elliptical slot. The FET switch can be actuated without battery, using solely the ambient RF power which is collected from a 5.8 GHz rectenna. Finally, **Figure 6c** presents a CPW-fed elliptical slot which uses a U-shaped slot with a microelectromechanical system (MEMS) switch to implement the frequency notch reconfigurability. The MEMS switch is actuated without bias lines, while for the application of the differential voltage for the reconfigurable UWB antennas presented in **Figure 6a** and **b**, bias lines with RF choke inductors are necessary. The MEMS switch was fabricated in-house [25], while the PIN diode and the FET switch are off-the-shelf components. (**Figure 7**) presents the measured S_{11} of three different reconfigurable UWB antennas that show successful implementation of a reconfigurable notch band at 5.8 GHz.

4. UWB antenna for chipless RFIDs

UWB monopoles are also used for the implementation of chipless UWB RFIDs [8]. Chipless tags are either backscattering-based or retransmission-based. Usually, UWB RFIDs are retransmission-based, and on-off keying (OOK) is performed by the presence or absence of a series of resonators which are coupled with the transmission line. Alternatively, the resonators may be perturbed and thus detuned by either short circuiting or open circuiting them. Backscattering occurs when a single antenna with high Q is used, while retransmission requires a second antenna which is preferably orthogonally polarized compared to the receiver, and it transmits a modulated signal after the unmodulated signal is received from the receiver antenna. The OOK modulation in chipless tags is performed in the frequency domain, and an
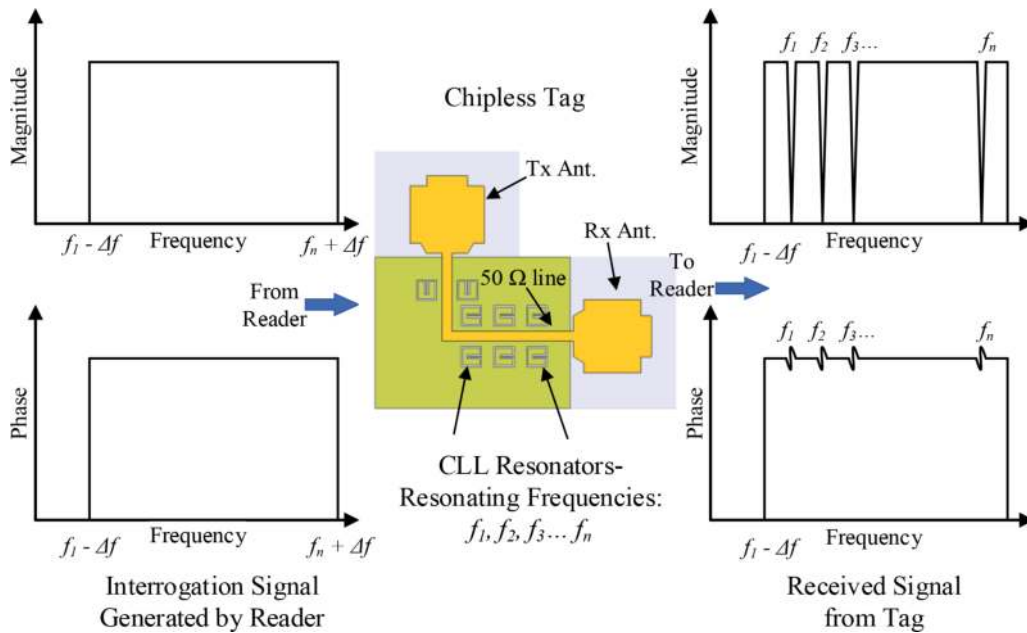
Figure 8.
Operation principle and schematic of chipless UWB RFIDs.

indicative signature of a retransmitted signal can be seen in **Figure 8**. The chipless UWB RFID schematic that is presented in **Figure 8** consists of a pair of UWB monopoles which are connected with a common feeding line. The feeding line is loaded with eight resonators forming an 8-bit word. Each resonator which has a slightly different size causes a frequency notch at a different frequency, and at the same time, it causes a phase discontinuity. With the use of a UWB interrogator, a wideband signal is sent, and the tag receives the signal, and it retransmits it back to the reader. The combination of resonators causes a unique electromagnetic signature, which identifies the tag. There is a variety of resonators that can be used, such as slits, CLLs, or slot ring resonators (SRRs). Batteryless, chipless, and entirely passive UWB RFIDs can be inkjet-printed on paper substrates and be massively and rapidly produced for disposable RFID tags, such as the baggage paper-based tags which are used to identify the checked-in luggage. A pair of microstrip-fed UWB monopole antennas is well-suited for the implementation of chipless UWB RFIDs.

5. UWB antennas for radar applications

In many types of radars such as GPR, through-wall imaging radars, or even breast imaging systems, UWB signals are required. For high-gain and high-power radars, end-fire UWB antennas are preferred because they perform with unidirectional, high gain which is necessary for enhanced radar range. Linearly tapered antennas (LTA) like Vivaldi antennas [26, 27] are widely used, and the more complex double exponentially tapered slot antennas (DETSA) can also be used. **Figure 9** presents a high-gain DETSA antenna fabricated on flexible liquid crystal polymer (LCP) substrate [28]. The implemented gain varies between 7 and 12 dBi. The use of flexible substrate such as LCP allows the adoption of the longitudinal antenna along a non-planar surface as can be seen in **Figure 9b**. End-fire DETSA has been shown to redirect the maximum gain direction along the tangent of the ending point; therefore, it can be used to implement high-gain directive radar front ends where two or even four DETSA antennas can be combined to form a confocal high-gain
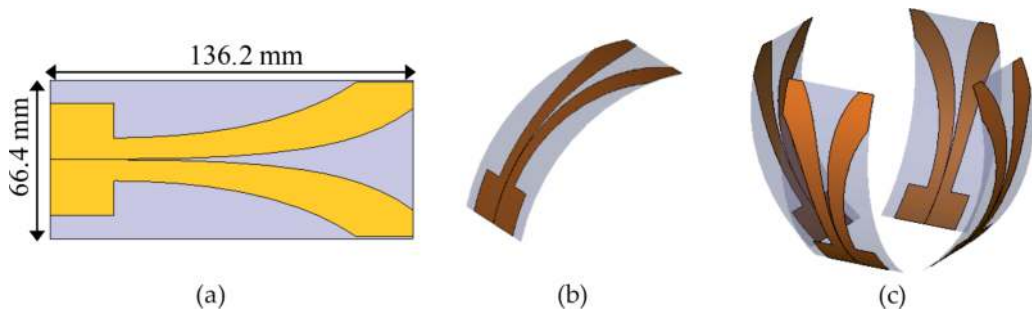
Figure 9.
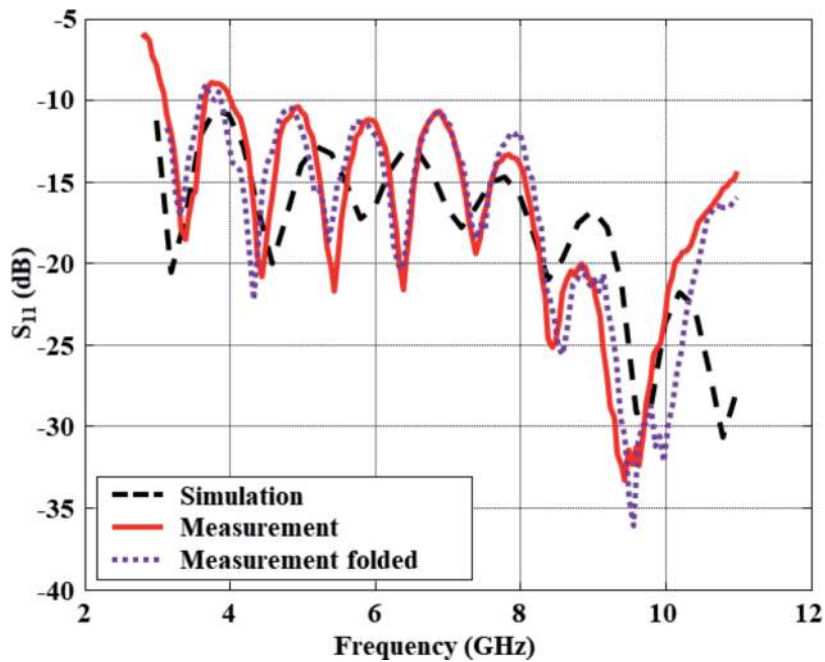*(a) Planar DETSA, (b) conformal DETSA, (c) DETSA antennas confocal array.*

Figure 10.
Simulated and measured S_{11} for planar and folded DETSA [22].

array as can be seen in **Figure 9c**. For GPR or through-wall imaging radars, a directive confocal array is placed about the ground target or on the wall. These radars are mono-static, and the same antenna system operates both as the transmitter and the receiver. It is desired to have high penetration capability which means that high-gain antennas and high-gain amplifiers are used to detect reflected signals propagating through high-loss media. End-fire high-gain antennas such as the Vivaldi antennas and their variations are usually used for these applications. In (**Figure 10**) it can be seen that good agreement is achieved between simulated and measured S11 and there is no difference between planar and folded DETSA return loss.

6. Conformal UWB antennas

In several occasions UWB antennas need to be integrated or mounted on non-planar surfaces, and consequently the use of conformal UWB antennas has been investigated by several researchers. In [22, 29] three distinct UWB antennas are used in order to test their matching and radiation characteristics when the antennas are

mounted on cylindrical surfaces of different radii. The first is a polygonal monopole antenna which will be referred to with the acronym PM for brevity. The second is a CPW-fed, elliptical slot antenna or ES for brevity, and finally a more compact size elliptical monopole or EM as it will be referred as, for brevity. Since one of the most popular solutions for a variety of UWB applications is the fat monopole, two such prototypes (PM and EM), significantly different in size, are investigated. Liquid crystal polymer (LCP) is used as fabrication substrate because LCP has relatively low dielectric constant (ε_r = 3) and low loss (tanδ = 0.002). For the two monopole antennas, the PM and the EM, the commercially available substrate, with thickness of 100 μm, is used. The fabricated prototypes are tested in planar shape and also when they are mounted on two different Styrofoam cylinders with radius either 25 or 15 mm. The used prototype antennas in planar shapes are presented in **Figure 11**.

The prototypes are measured in planar shape (R = inf), and then the measurements are repeated with the antennas mounted on custom-made cylinders with (a) radii 25 mm (R = 25 mm) and (b) 15 mm (R = 15 mm). The used cylinders were custom-made at a machine shop, and Styrofoam (ε_r = 1.03) material was used to resemble free space radiation conditions. When an antenna is kept in planar shape, it may be assumed that it is mounted on a cylinder with infinite radius, and this is the description (R = inf) used in the legends for the following figures. The measured S_{11} results for the three antennas are presented in **Figure 12**. In every one of the three cases presented in **Figure 11**, it can be observed that the measured reflection coefficient for the three different radius values is almost identical. Radiation pattern measurements can be also seen in **Figures 13–15**. Considering the high accuracy and the pattern measurements, in almost every compared pair of
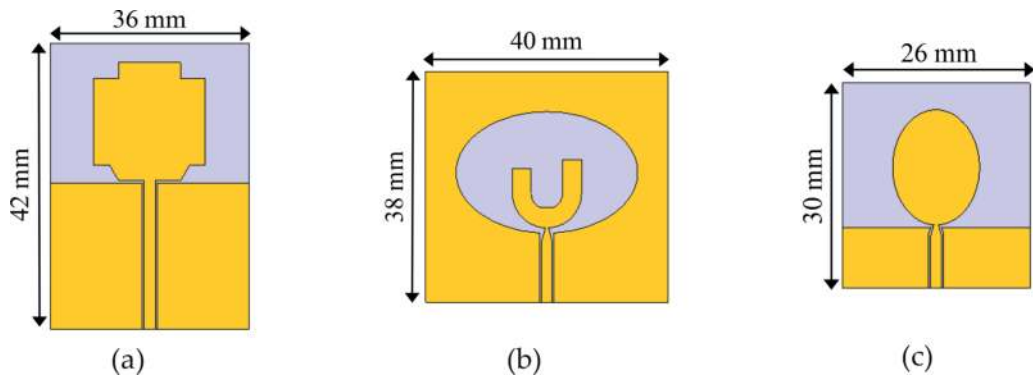

Figure 11.
Polygonal monopole (PM), elliptical slot (ES), and elliptical monopole (EM) UWB antennas in planar form.
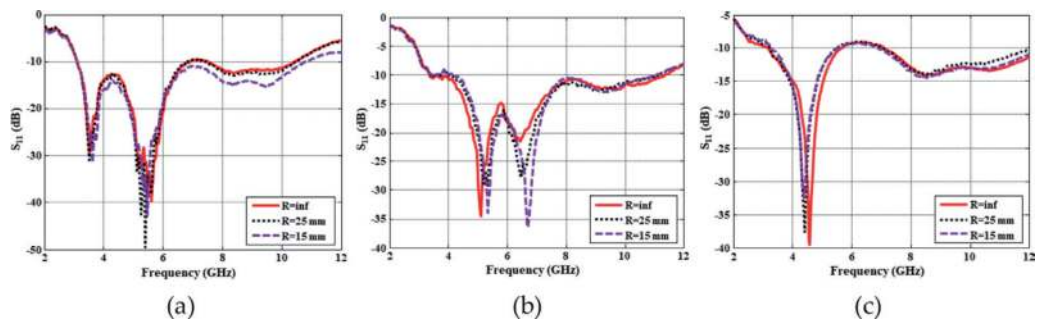

Figure 12.
Measured S_{11} under three different bending conditions for (a) polygonal monopole (PM), (b) elliptical slot (ES), and (c) elliptical monopole (EM) [22].
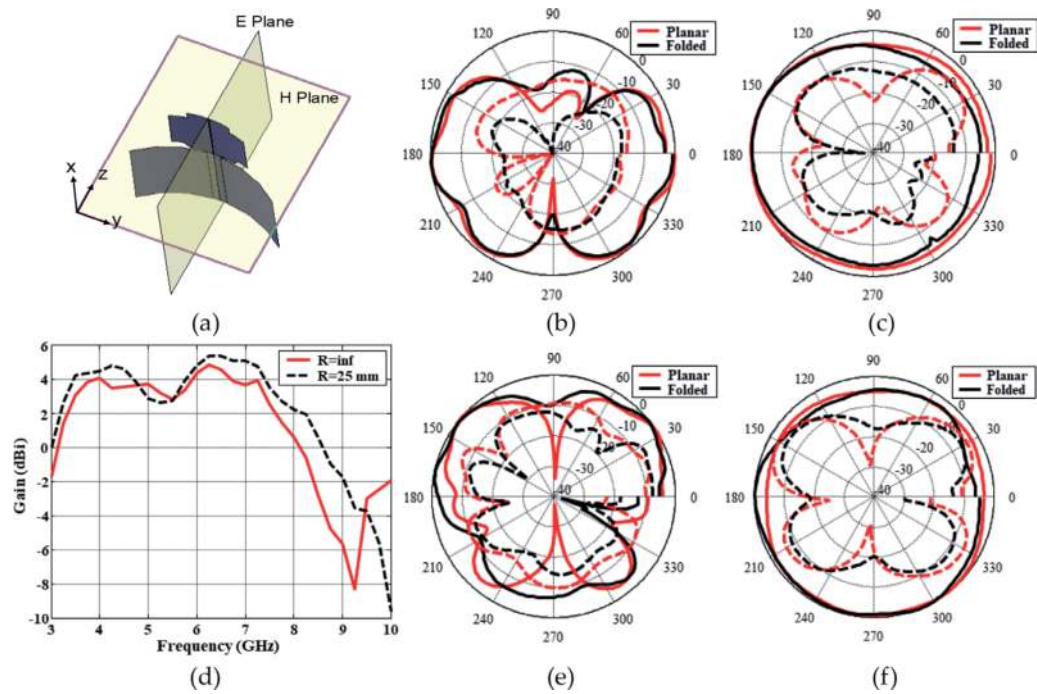
Figure 13.
Measured radiation patterns and gain for the polygonal monopole (PM) in planar form and when it is folded around a Styrofoam cylinder with a 25 mm radius. (a) Conformal PM, (b) E-plane at 5 GHz, (c) H-plane at 5 GHz, (d) measured gain (dBi) vs. frequency, (e) E-plane at 9 GHz, and (f) H-plane at 9 GHz [22].
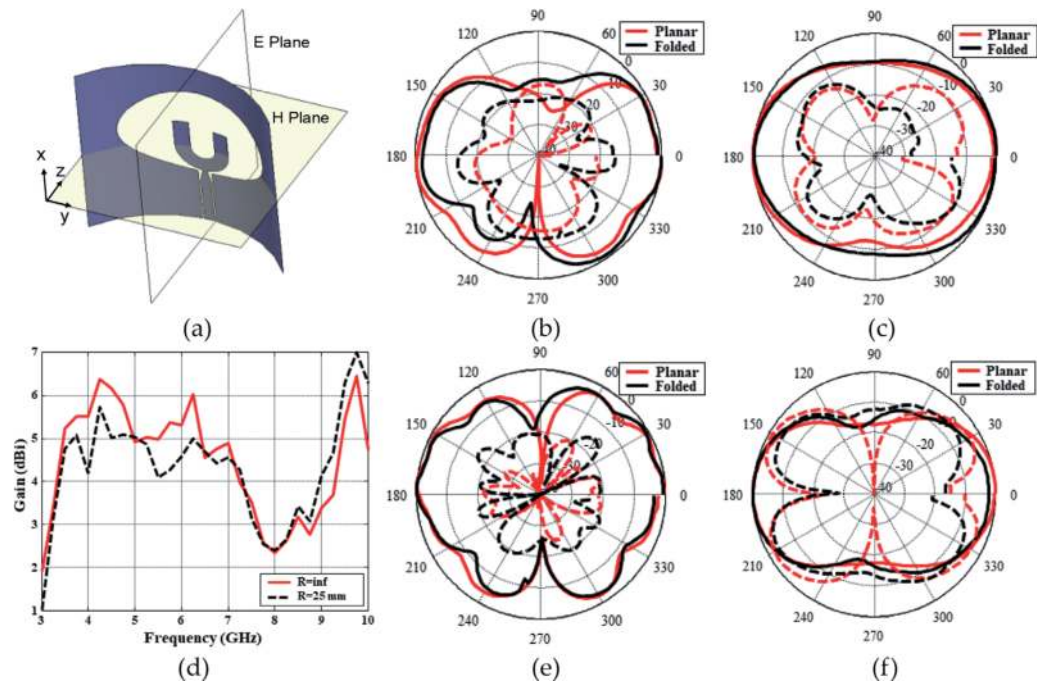

Figure 14.
Measured radiation patterns and gain for the elliptical monopole (EM) in planar form and when it is folded around a Styrofoam cylinder with a 25 mm radius. (a) Conformal EM radiator, (b) E-plane at 5 GHz, (c) H-plane at 5 GHz, (d) measured gain (dBi) vs. frequency, (e) E-plane at 9 GHz, and (f) H-plane at 9 GHz [22].

radiation patterns, the agreement between the patterns deduced from the planar and folded antennas is noteworthy. Both the shape of the patterns and the maximum directivity remain mostly steady, verifying the good agreement between the
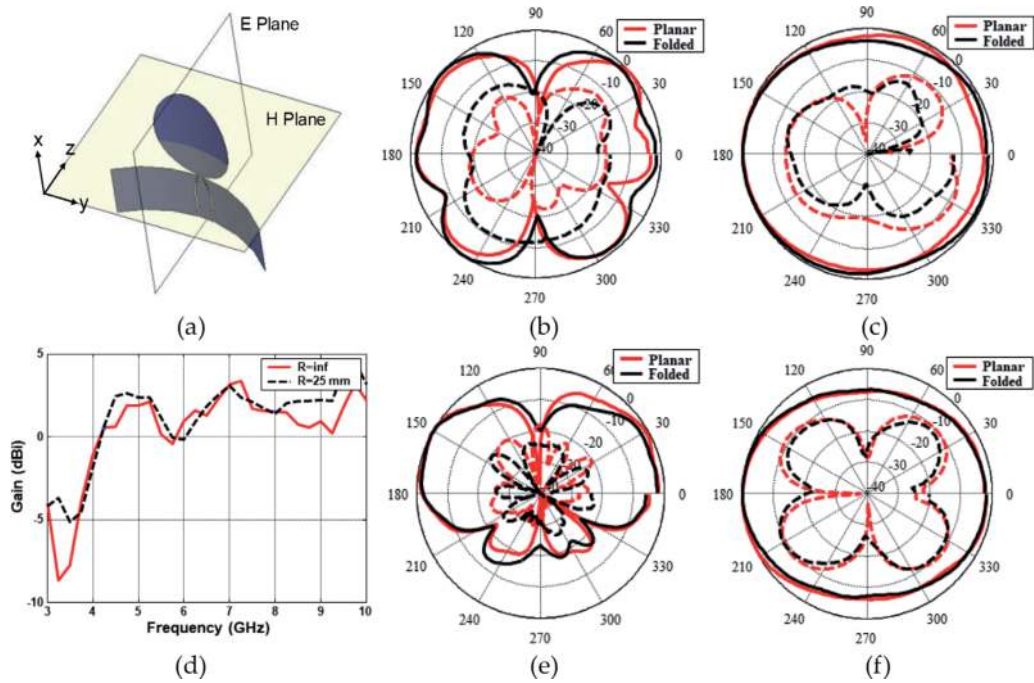
Figure 15.
Measured radiation patterns and gain for the elliptical monopole (EM) in planar form and when it is folded around a Styrofoam cylinder with a 25 mm radius. (a) EM radiator, (b) E-plane at 5 GHz, (c) H-plane at 5 GHz, (d) measured gain (dBi) vs. frequency, (e) E-plane at 9 GHz, and (f) H plane at 9 GHz [22].
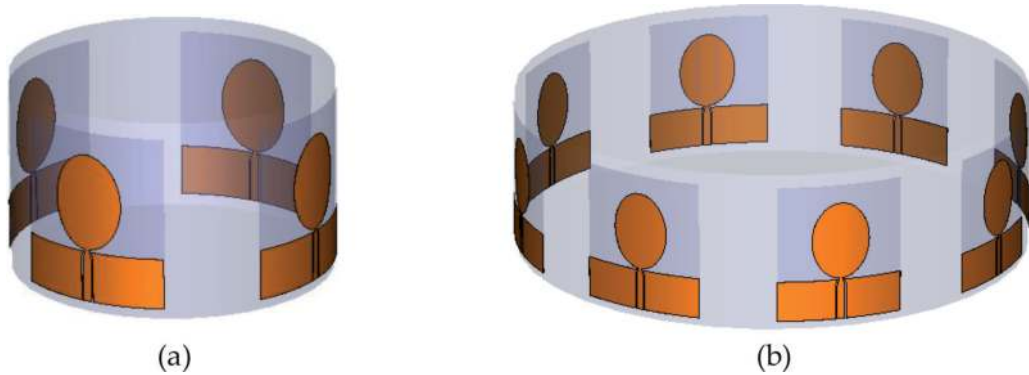

Figure 16.
Conformal cylindrical array of (a) four EM elements and (b) eights EM elements.

planar and folded antennas' radiation behavior. In conclusion and considering the testing results for all three prototypes, it can be claimed that the radiation patterns of omnidirectional UWB antennas are not significantly affected by conforming the antennas around a cylinder when the axis of the cylinder is parallel to the feeding line direction.

The use of conformal UWB antennas allows their direct use for the implementation of conformal cylindrical arrays. Such arrays are used for microwave imaging systems that are used for high-accuracy breast tumor detection devices that can be found in hospitals or even for wearable lightweight low-cost devices. **Figure 16** presents a schematic for the design of two cylindrical arrays that consist of four and eight conformal elliptical monopole UWB radiators, respectively. The radiated power is focused toward the axis of the cylinder, and the involved elements can radiate simultaneously, one at a time, or in various combinations implementing multistatic radars with different focus characteristics.
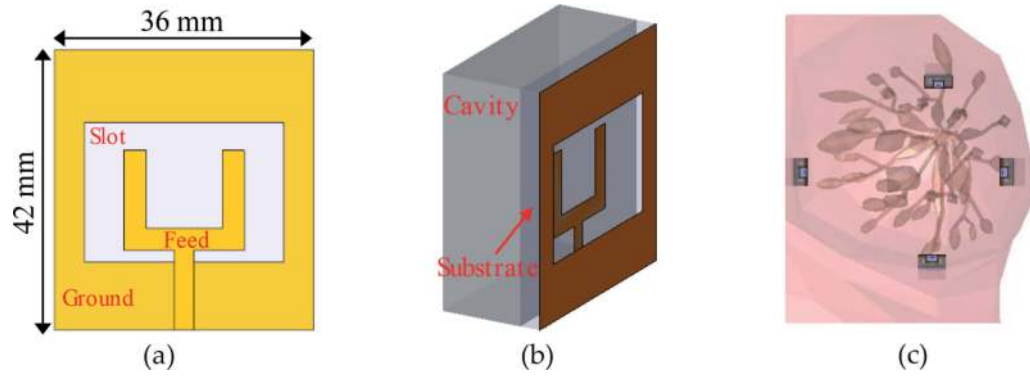
Figure 17.
(a) Cavity-backed slot UWB antenna, (b) prospective view, and (c) multiple elements in close proximity with a realistic breast phantom.

7. Microwave imaging radar antenna element

Recently microwave imaging was considered as an alternative promising technology for medical imaging especially since the required cost is much lower than the most prominent medical imaging methods such as computational tomography (CT) or magnetic resonance imaging (MRI). For the use of microwave imaging devices like the ones used for breast tumor detection in clinical trials [19, 20], the number or radiating elements is important. Generally, it is desired to use high number of elements which should have unidirectional radiation patterns, while the cross-coupling among the radiating elements must be as small as possible. As a result, the use of compact unidirectional UWB radiators is considered. An effective solution is the use of cavity-backed slot antennas. Such an element is presented in **Figure 17**. An implementation of a microwave imaging device consisting of similar such radiators is described in [21, 30]. The front face can be made conformal to better match the non-planar surface, while the feeding cable can pass through the metallic cavity that is used to cancel the back radiation. The desired low profile of the cavity and the intermediate gap between the radiating antenna elements and the target make the design of such an antenna a challenging task. In order to avoid additional reflections, the target is immersed in a liquid with controlled dielectric constant since the UWB antennas' matching can be severely degraded when the antenna radiates in close proximity or in touch with the human body. The high effect of the human body with the complex electromagnetic characteristics on the UWB antenna performance necessitates the use of accurate human phantoms in the full-wave simulations. **Figure 17c** demonstrates a cavity-backed slot UWB antenna in close proximity with a realistic breast phantom in a setup used in a full-wave simulator in order to ensure the good performance of the antenna when it radiates in close proximity with human body parts. Although the metallic cavity increases the profile of the receiver, it is very useful since it blocks signals which are not coming directly from the target.

Different vendors [19, 20] use customized UWB antennas which serve better the preferred reconstruction algorithms that they use; however, the presented cavity-backed slot radiator is one of the best candidates for medical microwave devices.

8. Conclusion

Selected UWB antennas for personal area network communication systems, for positioning and location tracking, and for numerous radar applications are presented. It is evident that depending on the application, different antenna

characteristics are required and different types of antennas are better suited. For wireless personal network devices, omnidirectional radiation patterns are preferred, and the compact size of the antenna with a low-profile planar design is the most useful, in most cases. There are several types of antennas that can be used; however, the monopole antenna is the most widely used design. Either CPW-fed or microstrip-fed UWB monopole is the most prominent solution. UWB monopoles have been used extensively for the implementation of reconfigurable UWB antennas which are capable of filtering out the interfering signals that share parts of the 3.1–10.6 GHz, FCC designated UWB spectrum. Frequency notch bands can be created with the addition of resonators which can be implemented on either the radiator or the feeding line or even the RF ground segments. Quarter-wavelength open stubs, half-wavelength linear segments, half-wavelength slots, and more complex in shape resonators, such as CLLs or SRRs, have been successfully used. For the reconfigurability attribution, RF switches are required, and depending on the resonator geometry and the biasing conditions, PIN diodes, FET switches, or MEMS switches can be used.

UWB antennas for positioning and tracking are used for both the interrogator and the RFID tags. Apparently different characteristics are needed for each case. For the interrogators high-gain, directive antennas with agile radiation patterns are preferred, while for the RFID tags, omnidirectional lightweight and low-cost antennas are needed. The RFIDs are often customized considering the electromagnetic characteristics of the items that they tag, and they can be either chipless or terminated with an IC load. The operation principle of chipless UWB RFIDs exploits the presence of a series of resonators which are coupled with the transmission line that connects the two antennas. One antenna receives the interrogator's signal, and the second one retransmits the modulated signal back to the reader. Chipless UWB RFIDs are entirely passive, and thus they can be easily fabricated using additive manufacturing technologies such as inkjet printing.

For radar applications, and depending on the target characteristics and the size and cost constraints, a wide variety of UWB antennas are used. For relatively long-range monostatic radars, such as ground-penetrating radars or through-wall imaging devices, high-gain directive antennas are used. Vivaldi antennas and their variations are the most common UWB antennas used for monostatic radars. For multistatic radars, like the ones used for microwave imaging for breast tumor detection, the requirements are very different. Since the target is relatively small and the size of the object under detection can be smaller than 1 cm^3, the radiators form a concave array. Cylindrical and hemispherical configurations are used, and the desired UWB antenna elements must have unidirectional radiation patterns, and they must be shielded from cross-coupling, while their size should be small to allow a large number of elements in a relatively small volume. Medical microwave imaging systems using UWB technology keep developing, and there are currently several vendors which have developed products which are cleared for clinical trials. Cavity-backed radiators are used covering different sub-bands in the UWB spectrum or even lower-frequency bands. These UWB antennas have conformal surfaces and are combined to form conformal arrays. They are co-designed with the human tissue target, since the radiation characteristics of UWB antennas change significantly when the antennas radiate in close proximity with the human body.

UWB antennas are integrated parts of devices which are used for a wide range of applications. For some applications, off-the-shelf UWB antennas can be successfully used or even antennas designed for similar scope, but for several other cases, UWB antennas must be customized and be co-designed with the surrounding environment since they can be easily mismatched and their assumed

performance can be significantly degraded. Therefore, for the successful design of an effective UWB antenna, the antenna must be simulated and tested in a realistic environment that must consider the characteristics of the adjacent media and the surrounding objects.

Conflict of interest

All authors listed have contributed sufficiently to the project to be included as authors. The authors declare that there is no conflict of interest, in terms of financial or other regarding the publication of this book chapter.

Author details

Symeon Nikolaou* and Abdul Quddious
Frederick University and Frederick Research Center, Nicosia, Cyprus

*Address all correspondence to: s.nikolaou@frederick.ac.cy

IntechOpen

References

[1] Nikolaou S, Abbasi MA. Design and development of a compact UWB monopole antenna with easily-controllable return loss. IEEE Transactions on Antennas and Propagation. 2017;**65**(4):2063-2067. DOI: 10.1109/TAP.2017.2670322

[2] Nikolaou S, Abbasi MA. Miniaturization of UWB antennas on organic material. International Journal of Antennas and Propagation. 2016;**2016**:12. DOI: 10.1155/2016/5949254. Article ID 5949254

[3] Tang MC, Wang H, Deng T, Ziolkowski RW. Compact planar ultrawideband antennas with continuously tunable, independent band-notched filters. IEEE Transactions on Antennas and Propagation. 2016;**64**(8):3292-3301. DOI: 10.1109/TAP.2016.2570254

[4] Ghahremani M, Ghobadi C, Nourinia J, Ellis MS, Alizadeh F, Mohammadi B. Miniaturised UWB antenna with dual-band rejection of WLAN/WiMAX using slitted EBG structure. IET Microwaves, Antennas and Propagation. 2018;**13**(3):360-366. DOI: 10.1049/iet-map.2018.5674

[5] Doddipalli S, Kothari A. Compact UWB antenna with integrated triple notch bands for WBAN applications. IEEE Access. 2019;**7**:183-190. DOI: 10.1109/ACCESS.2018.2885248

[6] Zhang J, Shen Z. Dual-band shared-aperture UHF/UWB RFID reader antenna of circular polarization. IEEE Transactions on Antennas and Propagation. 2018;**66**(8):3886-3893. DOI: 10.1109/TAP.2018.2839883

[7] Decarli N, Guidi F, Dardari D. Passive UWB RFID for tag localization: Architectures and design. IEEE Sensors Journal. 2016;**16**(5):1385-1397. DOI: 10.1109/JSEN.2015.2497373

[8] Liu J. Chipless UWB-RFID tag with spectral and temporal joint signatures. In: 2017 Sixth Asia-Pacific Conference on Antennas and Propagation (APCAP); 16 October 2017. pp. 1-3

[9] Galajda P, Pecovsky M, Gazda J, Drutarovsky M. Novel M-sequence UWB sensor for ground penetrating radar application. In: 2018 IEEE Asia-Pacific Conference on Antennas and Propagation (APCAP); 5 August 2018. pp. 110-111

[10] Liang J, Liu X, Liao K. Soil moisture retrieval using UWB echoes via fuzzy logic and machine learning. IEEE Internet of Things Journal. 2018;**5**(5):3344-3352. DOI: 10.1109/JIOT.2017.2760338

[11] Qi F, Liang F, Liu M, Lv H, Wang P, Xue H, et al. Position-information-indexed classifier for improved through-wall detection and classification of human activities using UWB bio-radar. IEEE Antennas and Wireless Propagation Letters. 2019;**18**(3): 437-441. DOI: 10.1109/LAWP.2019. 2893358

[12] Song Y, Hu J, Chu N, Jin T, Zhang J, Zhou Z. Building layout reconstruction in concealed human target sensing via UWB MIMO through-wall imaging radar. IEEE Geoscience and Remote Sensing Letters. 2018;**15**(8):1199-1203. DOI: 10.1109/LGRS.2018.2834501

[13] Shao W, Edalati A, McCollough TR, McCollough WJ. A time-domain measurement system for UWB microwave imaging. IEEE Transactions on Microwave Theory and Techniques. 2018;**66**(5):2265-2275. DOI: 10.1109/TMTT.2018.2801862

[14] Wang F. Assembly conformal antenna array for wearable microwave breast imaging application. In: Loughborough Antennas &

Propagation Conference (LAPC 2017); Loughborough; 2017. pp. 1-5

[15] Wang F, Arslan T, Wang G. Breast cancer detection with microwave imaging system using wearable conformal antenna arrays. In: 2017 IEEE International Conference on Imaging Systems and Techniques (IST); 18 October 2017. pp. 1-6

[16] Mukherjee S, Udpa L, Udpa S, Rothwell EJ, Deng Y. A Time reversal-based microwave imaging system for detection of breast tumors. IEEE Transactions on Microwave Theory and Techniques. May 2019;**67**(5):2062-2075. DOI: 10.1109/TMTT.2019.2902555

[17] Song H, Sasada S, Masumoto N, Kadoya T, Shiroma N, Orita M, et al. Detectability of breast tumors in excised breast tissues of Total mastectomy by IR-UWB-radar-based breast cancer imaging. IEEE Transactions on Biomedical Engineering. 17 Dec 2018: (Early access). DOI: 10.1109/TBME.2018.2887083

[18] Bourqui J, Sill JM, Fear EC. A prototype system for measuring microwave frequency reflections from the breast. Journal of Biomedical Imaging. 2012;**2012**:9. DOI: 10.1155/2012/851234

[19] Translational Medical Device Lab: Imaging and Diagnostics [Internet]. Available from: https://tmdlab.ie/ [Accessed: 24 April 2019]

[20] Micrima: Developing Technology for Breast Cancer Screening [Internet] Available from: https://micrima.com/ [Accessed: 24 April 2019]

[21] Porter E, Bahrami H, Santorelli A, Gosselin B, Rusch LA, Popović M. A wearable microwave antenna array for time-domain breast tumor screening. IEEE Transactions on Medical Imaging. 2016;**35**(6):1501-1509. DOI: 10.1109/TMI.2016.2518489

[22] Nikolaou S. Design and implementation of compact reconfigurable antennas for UWB and WLAN applications [Doctoral dissertation]. Georgia Institute of Technology; 2006

[23] Nikolaou S, Davidović M, Nikolić M, Vryonides P. Triple notch UWB antenna controlled by three types of resonators. In: 2011 IEEE International Symposium on Antennas and Propagation (APSURSI); 3 July 2011. pp. 1478-1481. DOI: 10.1109/APS.2011.5996574

[24] Quddious A, Ali M, Abbasi B, Vryonides P, Nikolaou S, Antoniades MA, et al. Reconfigurable notch-band UWB Antenna with RF-to-DC rectifier for dynamic reconfigurability. In: 2018 IEEE International Symposium on Antennas and Propagation & USNC/URSI National Radio Science Meeting; 8 July 2018. pp. 283-284. DOI: 10.1109/APUSNCURSINRSM.2018.860868

[25] Nikolaou S, Kingsley ND, Ponchak GE, Papapolymerou J, Tentzeris MM. UWB elliptical monopoles with a reconfigurable band notch using MEMS switches actuated without bias lines. IEEE Transactions on Antennas and Propagation. 2009;**57**(8):2242-2251. DOI: 10.1109/TAP.2009.2024450

[26] Zhang C, Hu Y, Jin X, Huang X. High performance linearly tapered slot antenna (ltsa) using parasitic patch. In: 2017 Sixth Asia-Pacific Conference on Antennas and Propagation (APCAP); 16 October 2017. pp. 1-3

[27] Zhang F, Zhang FS, Zhao G, Lin C, Jiao YC. A loaded wideband linearly tapered slot antenna with broad beamwidth. IEEE Antennas and Wireless Propagation Letters. 2011;**10**:79-82. DOI: 10.1109/LAWP.2011.2106477

[28] Nikolaou S, Ponchak GE, Papapolymerou J, Tentzeris MM.

Conformal double exponentially tapered slot antenna (DETSA) on LCP for UWB applications. IEEE Transactions on Antennas and Propagation. 2006;**54**(6):1663-1669. DOI: 10.1109/TAP.2006.875915

[29] Nikolaou S, Tentzeris MM, Papapolymerou J. Study of a conformal UWB elliptical monopole antenna on flexible organic substrate mounted on cylindrical surfaces. In: 2007 IEEE 18th International Symposium on Personal, Indoor and Mobile Radio Communications; 3 September 2007. pp. 1-4

[30] Gibbins D, Klemm M, Craddock I, Preece A, Leendertz J, Benjamin R. Design of a UWB wide-slot antenna and a hemispherical array for breast imaging. In: 2009 3rd European Conference on Antennas and Propagation; 23 March 2009. pp. 2967-2970